Ruthenium and Rhodium Complexes with Thiolate-Containing Pincer Ligands Produced by C−S Bond Cleavage of Pyridyl-Substituted Dibenzothiophenes

Mayuko Shibue, Masakazu Hirotsu,* Takanori Nishioka, and Isamu Kinoshita

Department of Material Science, Graduate School of Science, Osaka City University, Sumiyoshi-ku, Osaka 558-8585, Japan

Received May 2, 2008

Treatment of 4-(2′-pyridyl)dibenzothiophene (PyDBT) with the ruthenium carbonyl cluster $[Ru_3(CO)_{12}]$ gave the diruthenium(II) complex $[Ru(\mu\text{-PyBPT-}\kappa^3N,C,S)(CO)_2]_2$ (**1**), where PyBPT denotes a dianion of 3′-(2″-pyridyl)-1,1′-biphenyl-2-thiol. The tridentate-*N,C,S* PyBPT ligand provides a pincer structure consisting of a six-membered thiaruthenacycle and a five-membered azaruthenacycle. The thiolate-containing NCS pincer ligand in **1** is produced by cleavage of a carbon−sulfur bond adjacent to a pyridyl group in PyDBT. The corresponding reactions using 4-(4′-methyl-2′-pyridyl)dibenzothiophene (4-MePyDBT) and 4-(6′-methyl-2′-pyridyl)dibenzothiophene (6-MePyDBT) afforded the diruthenium(II) complexes with the same pincer framework $[Ru(\mu\text{-4-MePyBPT-}\kappa^3N,C,S)(CO)_2]_2$ (**2**) and $[Ru(\mu\text{-6-MePyBPT-}\kappa^3N,C,S)(CO)_2]_2$ (**3**), respectively. The much slower formation of **3** certifies the reaction path through the initial coordination of the pyridyl group to Ru or the formation of an N,S-chelate structure. Indeed, PyDBT showed the chelating ability in the ruthenium(II) complex $[Ru(\eta^6\text{-}C_6H_6)(PyDBT\text{-}\kappa^2N,S)Cl]CF_3SO_3$ (**4**). Complex **1** contains C_i and C_2 symmetrical isomers, **1a** and **1b**, respectively, which were separated. The latter isomerized to **1a** in DMSO-d_6 at 80 °C. The stepwise formation of the same NCS pincer ligand was established in the reaction of $[Rh(\mu\text{-Cl})(CO)_2]_2$ with PyDBT. The facile reaction at room temperature produced the mononuclear rhodium(I) complex *cis*-$[RhCl(CO)_2(\eta^1\text{-}N\text{-PyDBT})]$ (**5**). The isolated complex **5** was converted to the tetranuclear rhodium(I/III/III/I) complex $[\{Rh(\mu\text{-PyBPT-}\kappa^3N,C,S)\}(\mu\text{-Cl})_2\{Rh(CO)_2\}]_2$ (**6**) at 100 °C for 3 days.

Introduction

Metal-mediated activation of strong bonds, such as C−C, C−H, C−O, and C−X (X = halogen), is a vital research area related to the catalytic transformation of organic molecules.[1,2] Carbon−sulfur bonds are also activated on metal centers to provide useful reaction pathways for novel sulfur-containing compounds.[1d,3] The C−S bond cleavage of thiophenes is an industrially important process in catalytic hydrodesulfurization (HDS) that removes sulfur from organosulfur compounds in petroleum feedstocks.[4] The research on HDS of thiophenes gave various metallacyclic compounds having thiolato-S coordination in addition to valuable insights about the C−S bond cleavage.[5−8] The reactions of dibenzothiophenes (DBT) with organometallic compounds are of particular interest because dibenzothiophenes are especially resistant to desulfurization, which causes serious problems for further HDS.[7,8] The rich sulfur−metal chemistry originating from HDS would provide new ways to produce S-containing functional materials. In this context, we started research on the metallacyclic compounds with a pincer frame derived from dibenzothiophenes via the C−S cleavage reaction.

* To whom correspondence should be addressed. Tel: +81-6-6605-2546. Fax: +81-6-6690-2753. E-mail: mhiro@sci.osaka-cu.ac.jp.

(1) (a) Dyker, G. *Angew. Chem., Int. Ed.* **1999**, *38*, 1698–1712. (b) Crabtree, R. H. *J. Chem. Soc., Dalton Trans.* **2001**, 2437–2450. (c) Lersch, M.; Tilset, M. *Chem. Rev.* **2005**, *105*, 2471–2526. (d) Goj, L. A.; Lail, M.; Pittard, K. A.; Riley, K. C.; Gunnoe, T. B.; Petersen, J. L. *Chem. Commun.* **2006**, 982–984.

(2) (a) Albrecht, M.; van Koten, G. *Angew. Chem., Int. Ed.* **2001**, *40*, 3750–3781. (b) van de Boom, M. E.; Milstein, D. *Chem. Rev.* **2003**, *103*, 1759–1792.

(3) (a) Mullen, G. E. D.; Went, M. J.; Wocadlo, S.; Powell, A. K.; Blower, P. J. *Angew. Chem., Int. Ed. Engl.* **1997**, *36*, 1205–1207. (b) Li, M.; Ellern, A.; Espenson, J. H. *J. Am. Chem. Soc.* **2005**, *127*, 10436–10447. (c) Cabeza, J. A.; del Río, I.; Sánchez-Vega, M. G.; Suárez, M. *Organometallics* **2006**, *25*, 1831–1834. (d) Schaub, T.; Backes, M.; Radius, U. *Chem. Commun.* **2007**, 2037–2039.

(4) (a) Bej, S. K.; Maity, S. K.; Turaga, U. T. *Energy Fuels* **2004**, *18*, 1227–1237. (b) Mochida, I.; Choi, K.-H. *J. Jpn. Petrol. Inst.* **2004**, *47*, 145–163.

(5) (a) Angelici, R. J. *Coord. Chem. Rev.* **1990**, *105*, 61–76. (b) Rauchfuss, T. B. *Prog. Inorg. Chem.* **1991**, *39*, 259–329. (c) Bianchini, C.; Meli, A. *Acc. Chem. Res.* **1998**, *31*, 109–116. (d) Chen, J.; Angelici, R. J. *Coord. Chem. Rev.* **2000**, *206−207*, 63–99. (e) Angelici, R. J. *Organometallics* **2001**, *20*, 1259–1275.

(6) (a) Arce, A. J.; Arrojo, P.; Deeming, A. J.; Sanctis, Y. D. *J. Chem. Soc., Dalton Trans.* **1992**, 2423–2424. (b) Mills, R. C.; Abboud, K. A.; Boncella, J. M. *Chem. Commun.* **2001**, 1506–1507. (c) Atesin, T. A.; Jones, W. D. *Organometallics* **2008**, *27*, 53–60.

(7) (a) Jones, W. D.; Chin, R. M. *J. Am. Chem. Soc.* **1992**, *114*, 9851–9858. (b) Garcia, J. J.; Mann, B. E.; Adams, H.; Bailey, N. A.; Maitlis, P. M. *J. Am. Chem. Soc.* **1995**, *117*, 2179–2186. (c) Vicic, D. A.; Jones, W. D. *J. Am. Chem. Soc.* **1997**, *119*, 10855–10856. (d) Dullaghan, C. A.; Zhang, X.; Greene, D. L.; Carpenter, G. B.; Sweigart, D. A.; Camiletti, C.; Rajaseelan, E. *Organometallics* **1998**, *17*, 3316–3322. (e) Vicic, D. A.; Jones, W. D. *Organometallics* **1998**, *17*, 3411–3413. (f) Vicic, D. A.; Jones, W. D. *J. Am. Chem. Soc.* **1999**, *121*, 7606–7617. (g) Yu, K.; Li, H.; Watson, E. J.; Virkaitis, K. L.; Carpenter, G. B.; Sweigart, D. A. *Organometallics* **2001**, *20*, 3550–3559. (h) McKinley, S. G.; Vecchi, P. A.; Ellern, A.; Angelici, R. J. *Dalton Trans.* **2004**, 788–793. (i) Vecchi, P. A.; Ellern, A.; Angelici, R. J. *Organometallics* **2005**, *24*, 2168–2176. (j) Torres-Nieto, J.; Arévalo, A.; García, J. J. *Organometallics* **2007**, *26*, 2228–2233.

(8) (a) Bianchini, C.; Jiménez, M. V.; Meli, A.; Moneti, S.; Vizza, F.; Herrera, V.; Sánchez-Delgado, R. A. *Organometallics* **1995**, *14*, 2342–2352. (b) Myers, A. W.; Jones, W. D. *Organometallics* **1996**, *15*, 2905–2917. (c) Matsubara, K.; Okamura, R.; Tanaka, M.; Suzuki, H. *J. Am. Chem. Soc.* **1998**, *120*, 1108–1109. (d) Chen, J.; Angelici, R. J. *Organometallics* **1999**, *18*, 5721–5724. (e) Reynolds, M. A.; Guzei, I. A.; Angelici, R. J. *Organometallics* **2001**, *20*, 1071–1078. (f) Chehata, A.; Oviedo, A.; Arévalo, A.; Bernès, S.; García, J. J. *Organometallics* **2003**, *22*, 1585–1587.

10.1021/om8003916 CCC: $40.75
Publication on Web 08/05/2008

Chart 1

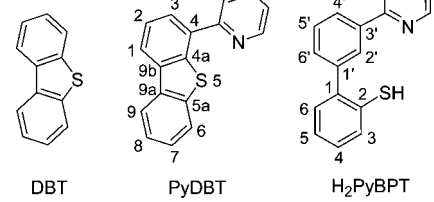

Scheme 1

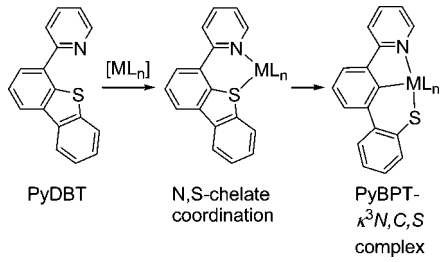

The target pincer-type complexes have recently attracted great interest because of their catalytic properties on C−C bond forming reactions, alkene dehydrogenation, transfer hydrogenation, and aldol reactions.[2,9] The most frequently studied pincer complexes have one central M−C bond supported by the coordination of two neutral 2*e* donor atoms (E) trans to each other, and their complexes are called "ECE pincer-type complexes". The steric and electronic environments of the metal centers can be tuned by changing the E donor atoms and their substituents. Moreover, the pincer-type complexes with high thermal stability offer significant advantage in catalytic reactions. Although the thiolato-S donor is quite important in artificial catalysts as well as in metalloenzymes, thiolate-containing pincer ligands have not been developed.[10,11]

The cyclometalation via the regioselective activation of C−H and C−X bonds has been a successful method for preparing pincer-type complexes.[2,9] The C−S cleavage reactions of dibenzothiophenes by metal compounds give thiametallacycles, even though it often includes side reactions by C−H activation, nonselective C−S activation, or desulfurization.[8] In this work, we have used pyridyl-substituted dibenzothiophenes, 4-(2′-pyridyl)dibenzothiophene (PyDBT) and its derivatives, as ligand precursors in order to facilitate the metalation reaction (Chart 1, Scheme 1). PyDBT can act as a monodentate ligand or a bidentate-*N,S* ligand, forming a six-membered chelate ring. Futhermore, the insertion of a metal center into the C−S bond on the pyridyl-substituted benzene ring provides a pincer frame consisting of a thiametallacycle and an azametallacycle: the formed tridentate-*N,C,S* ligand, PyBPT, is a dianion of 3′-(2″-pyridyl)-1,1′-biphenyl-2-thiol. We now report the syntheses of dinuclear ruthenium(II) and tetranuclear rhodium(I/III/III/I) complexes having the thiolate-containing pincer ligand PyBPT. As a result, we demonstrate that the coordination of the pyridyl group becomes an effective initial step for regioselective C−S bond cleavage.

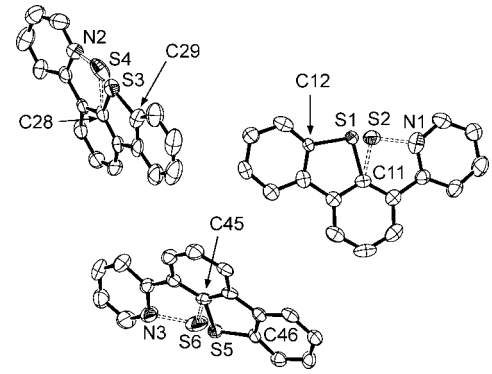

Figure 1. ORTEP drawing of PyDBT with thermal ellipsoids at the 50% probability level. Hydrogen atoms are omitted for clarity. Selected bond lengths (Å): C(11)−S(1) 1.783(3), C(11)−S(2) 1.763(4), C(28)−S(3) 1.758(4), C(29)−S(3) 1.755(4), C(45)−S(5) 1.759(3), C(46)−S(5) 1.756(3).

Results and Discussion

Syntheses of Pyridyl-Substituted Dibenzothiophenes. Three pyridyl-substituted dibenzothiophenes, PyDBT, 4-(4′-methyl-2′-pyridyl)dibenzothiophene (4-MePyDBT), and 4-(6′-methyl-2′-pyridyl)dibenzothiophene (6-MePyDBT), were prepared by the palladium-catalyzed cross-coupling reaction between dibenzothiophene-4-boronic acid and 2-bromopyridine derivatives according to a similar method described in the literature.[12] The structure of PyDBT was determined by single-crystal X-ray analysis. The asymmetric unit consists of three independent molecules that have similar structural features (Figure 1). The dibenzothiophene and pyridine rings connected by a C−C single bond are almost in a plane. All independent units were disordered by the flipped PyDBT molecule. Structural parameters for the dibenzothiophene part of PyDBT are similar to those observed for dibenzothiophene.[13]

Reactions of [$Ru_3(CO)_{12}$] with Pyridyl-Substituted Dibenzothiophenes. The ruthenium carbonyl cluster [$Ru_3(CO)_{12}$] (1 equiv) reacted with PyDBT (3 equiv) in toluene at 100 °C for 3 days to afford a pale yellow precipitate of [Ru(μ-PyBPT-κ^3*N,C,S*)$(CO)_2$]$_2$ (**1**) in 74% yield (Scheme 2). The ^{1}H NMR spectrum of **1** showed that the precipitate is a mixture of two isomers, **1a** and **1b**: the formation ratio was 1:1. The two isomers were separated by using dichloromethane, which predominantly dissolves **1b**.

Single-crystal X-ray analysis confirmed that both **1a** and **1b** have a dimeric structure consisting of two Ru(PyBPT)$(CO)_2$ units, one of which is observed in the asymmetric unit of each crystal (Figure 2). Selected bond lengths and angles are listed in Table 1. The structures of independent halves in **1a** and **1b** are similar to each other, but the overall structures provide symmetrical isomers: **1a** has C_i symmetry, while **1b** has C_2. Ruthenium is inserted into a C−S bond adjacent to a pyridyl group in PyDBT to form a six-membered thiaruthenacycle. A five-membered azaruthenacycle simultaneously formed by the coordination of the pyridyl group to complete a novel tridentate-*N,C,S* dianion ligand, PyBPT. Two Ru centers are bridged by two thiophenolato S atoms from the PyBPT ligands, and the

(9) (a) Gossage, R. A.; van de Kuil, L. A.; van Koten, G. *Acc. Chem. Res.* **1998**, *31*, 423–431. (b) Singleton, J. T. *Tetrahedron* **2003**, *59*, 1837–1857. (c) Zhao, J.; Goldman, A. S.; Hartwig, J. F. *Science* **2005**, *307*, 1080–1082.

(10) (a) Arink, A. M.; Braam, T. W.; Keeris, R.; Jastrzebski, J. T. B. H.; Benhaim, C.; Rosset, S.; Alexakis, A.; van Koten, G. *Org. Lett.* **2004**, *6*, 1959–1962. (b) Nishibayashi, Y.; Shinoda, A.; Miyake, Y.; Matsuzawa, H.; Sato, M. *Angew. Chem., Int. Ed.* **2006**, *45*, 4835–4839.

(11) (a) Evans, D. J.; Pickett, C. J. *Chem. Soc. Rev.* **2003**, *32*, 268–275. (b) Rao, P. V.; Holm, R. H. *Chem. Rev.* **2004**, *104*, 527–559. (c) Liu, X.; Ibrahim, S. K.; Tard, C.; Pickett, C. J. *Coord. Chem. Rev.* **2005**, *249*, 1641–1652.

(12) (a) Miyaura, N.; Yanagi, T.; Suzuki, A. *Synth. Commun.* **1981**, *11*, 513–519. (b) Reich, H. J.; Gudmundsson, B. Ö.; Green, D. P.; Bevan, M. J.; Reich, I. L. *Helv. Chim. Acta* **2002**, *85*, 3748–3772. (c) Kondolff, I.; Doucet, H.; Santelli, M. *J. Mol. Catal. A* **2007**, *269*, 110–118.

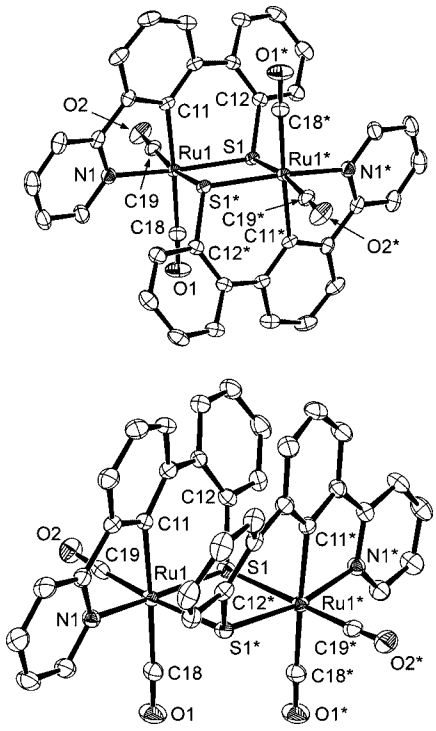

Figure 2. ORTEP drawings of **1a** (top) and **1b** (bottom) with thermal ellipsoids at the 50% probability level. Hydrogen atoms are omitted for clarity.

Table 1. Selected Bond Lengths (Å) and Angles (deg) for 1a and 1b

	1a	1b
Ru(1)−S(1)	2.3553(7)	2.3540(6)
Ru(1)−S(1*)	2.4683(7)	2.4822(5)
Ru(1)−N(1)	2.105(2)	2.105(2)
Ru(1)−C(11)	2.074(2)	2.087(2)
Ru(1)−C(18)	1.955(3)	1.950(2)
Ru(1)−C(19)	1.873(3)	1.862(2)
S(1)−C(12)	1.781(2)	1.776(2)
Ru(1)···Ru(1*)	3.6211(3)	3.6319(8)
S(1)−Ru(1)−S(1*)	82.72(2)	82.64(2)
S(1)−Ru(1)−N(1)	164.75(8)	167.69(5)
S(1)−Ru(1)−C(11)	91.47(8)	92.68(7)
N(1)−Ru(1)−C(11)	79.88(10)	79.89(9)
Ru(1)−S(1)−Ru(1*)	97.28(2)	97.32(2)
Ru(1)−S(1)−C(12)	108.48(10)	110.51(8)

remaining two coordination sites, which are cis to each other, are occupied by carbonyl ligands. The Ru−C(carbonyl) bond trans to C(carbanion) is longer than that trans to the bridging S atom by 0.082(3) Å for **1a** and 0.088(2) Å for **1b**. This is attributable to the trans influence induced by the strong σ-donating character of the carbanion C donor, showing Ru−C(carbanion) distances of 2.074(2) and 2.087(2) Å, respectively. The biphenyl moiety of the six-membered thiaruthenacycle in PyBPT shows a twisted structure: the dihedral angles between the two least-squares planes of the benzene rings are 31.15(12)° and 27.87(10)° for **1a** and **1b**, respectively. These twists are similar to those of *cis*- and *trans*-[Cp*Rh(μ-$SC_{12}H_8$)]$_2$ (26−29°) but are smaller than those observed for most other C−S insertion complexes of dibenzothiophenes.[7a,c,e,f,8b]

The corresponding reactions using 4-MePyDBT or 6-MePyDBT instead of PyDBT were carried out under similar conditions. The reaction of [$Ru_3(CO)_{12}$] with 4-MePyDBT produced pale yellow crystals of [Ru(μ-4-MePyBPT-κ^3*N,C,S*)$(CO)_2$]$_2$ (**2**) in 52% yield, while the reaction using 6-MePyDBT afforded a small amount of thin, pale yellow crystals of [Ru(μ-6-MePyBPT-κ^3*N,C,S*)$(CO)_2$]$_2$ (**3**) in 29% yield. The X-ray analysis of **2** showed a C_2 symmetrical diruthenium structure, depicted in Figure 3. The biphenyl twist of **2** (26.64(9)° and 27.28(8)°) was found to be similar to that of C_2 isomer **1b** (27.87(10)°) rather than C_i isomer **1a** (31.15(12)°). Although crystals of **3** were not suitable for single-crystal X-ray structure analysis, the preliminary results showed that **3** has a C_i symmetrical structure like **1a**.[14] The C_i and C_2 symmetrical isomers corresponding to **1a** and **1b**, respectively, are possible for both **2** and **3**. The solubility of **2** and **3** was not enough for NMR measurements, except that **2** was slightly soluble in dimethyl sulfoxide. Interestingly, the ^{1}H NMR spectrum of **2** in DMSO-d_6 showed only one set of signals, and their chemical shifts were similar to those of the C_2 isomer **1b**. Complex **3** was barely dissolved in DMSO-d_6 by heating at 80 °C, giving complicated signals in the ^{1}H NMR spectrum. The major signals were assignable to the coordinated 6-MePyBPT ligand in the C_i isomer of **3** on the basis of the chemical shifts, but isomerization is possible in the heating process (vide infra).

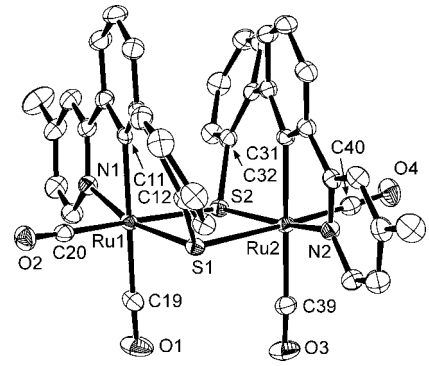

Figure 3. ORTEP drawing of **2** with thermal ellipsoids at the 50% probability level. Hydrogen atoms are omitted for clarity. Selected bond lengths (Å): Ru(1)−S(1) 2.3479(4), Ru(1)−S(2) 2.4859(5), Ru(1)−N(1) 2.1033(14), Ru(1)−C(11) 2.086(2), Ru(1)−C(19) 1.961(2), Ru(1)−C(20) 1.865(2), Ru(2)−S(1) 2.4812(5), Ru(2)−S(2) 2.3528(4), Ru(2)−N(2) 2.1027(14), Ru(2)−C(31) 2.089(2), Ru(2)−C(39) 1.950(2), Ru(2)−C(40) 1.865(2), Ru(1)···Ru(2) 3.6198(2).

The analogous C−S cleavage reaction of dibenzothiophene with [$Ru_3(CO)_{12}$] has been reported and produces the biphenyl-coordinated diruthenium complex [$Ru_2(\eta^2$-*C,C*-$C_{12}H_8)(\mu$-CO-$)(CO)_5$], in which dibenzothiophene is desulfurized by cleaving two C−S bonds to afford a five-membered ruthenacycle.[8f] This is quite different from our results: a single C−S bond activation leads to a six-membered thiaruthenacycle in **1**. The reactivity difference implies that the pyridyl substituent prevents the desulfurization by forming a five-memberd azaruthenacycle simultaneously. This cyclometalation would be critical to stabilize the tridentate-*N,C,S* coordination of C−S cleaved PyDBT, as inferred from the fact that many stable ruthenium

(13) Wright, J. D.; Ahmad, Z. A. *Acta Crystallogr.* **1981**, *B37*, 1848–1852.

(14) Crystallographic data for **3**: $C_{40}H_{26}N_2O_4Ru_2S_2$, fw = 864.92, size 0.18 × 0.07× 0.07 mm, monoclinic, space group $P2_1/n$, a = 9.329(6) Å, b = 18.083(11) Å, c = 10.169(7) Å, β = 105.704(13)°, V = 1651.5(18) Å^3, Z = 2, T = 193 K, D_{calcd} = 1.739 Mg/m^3, μ = 1.089 mm^{-1}, $F(000)$ = 864, refinement method full-matrix least squares on F^2, R1 (observed data with $I > 2\sigma(I)$) = 0.109, wR2 (all data) = 0.335, GOF = 1.001.

(15) (a) Reveco, P.; Medley, J. H.; Garber, A. R.; Bhacca, N. S.; Selbin, J. *Inorg. Chem.* **1985**, *24*, 1096–1099. (b) Hiraki, K.; Koizumi, M.; Kira, S.; Kawano, H. *Chem. Lett.* **1998**, 47–48. (c) Fernandez, S.; Pfeffer, M.; Ritleng, V.; Sirlin, C. *Organometallics* **1999**, *18*, 2390–2394. (d) Ryabov, A. D.; Lagadec, R. L.; Estevez, H.; Toscano, R. A.; Hernandez, S.; Alexandrova, L.; Kurova, V. S.; Fischer, A.; Sirlin, C.; Pfeffer, M. *Inorg. Chem.* **2005**, *44*, 1626–1634.

Scheme 2

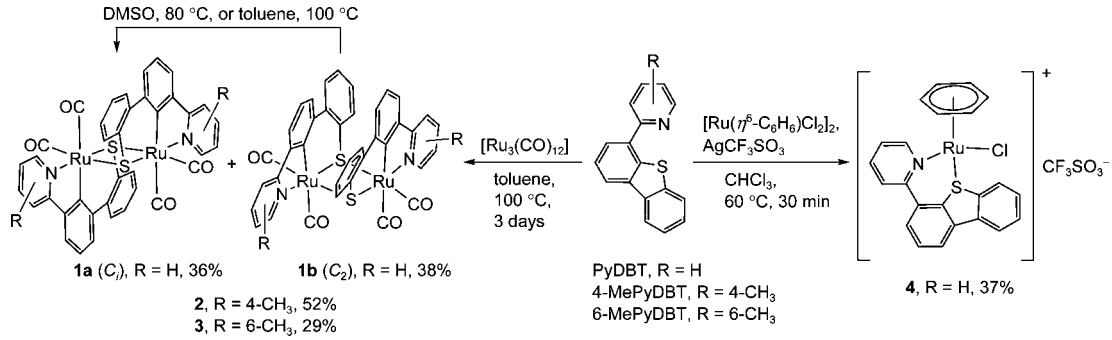

complexes with η^2-*N,C*-phenylpyridines have been synthesized by cyclometalation.[15]

Formation Mechanism of 1. The formation process of **1** from PyDBT and $[Ru_3(CO)_{12}]$ was investigated by the ^{1}H NMR experiments in toluene-d_8. Although transient species were observed in the NMR spectra, they have not been isolated yet.[16] The initial coordination of a pyridyl group or the N,S-chelate ring formation would be important because a C−S bond adjacent to the pyridyl group is selectively cleaved to form **1a** and **1b**. Furthermore, the reaction of 6-MePyDBT with $[Ru_3(CO)_{12}]$ is much slower than that of PyDBT: the reaction at 100 °C in toluene-d_8 was monitored by ^{1}H NMR, and a slight decrease of 6-MePyDBT was observed after 24 h.[16] Indeed, the isolated yield of complex **3** was lower than that of **1** or **2**. This demonstrates that the 6-positioned methyl group on the pyridyl group prevents the coordination of the pyridine N atom to a Ru center.

The N,S-chelate coordination of PyDBT, which forms a six-membered ring, provides a possible intermediate in the oxidative addition of the C−S bond. In order to confirm the chelate structure, according to Scheme 2, PyDBT was treated with $[RuCl(\mu\text{-}Cl)(\eta^6\text{-}C_6H_6)]_2$ in the presence of $AgCF_3SO_3$ to afford the N,S-chelated compound $[Ru(\eta^6\text{-}C_6H_6)(PyDBT\text{-}\kappa^2N,S)Cl]\text{-}CF_3SO_3$ (**4**). The X-ray crystal structure analysis showed that the asymmetric unit includes two independent complex cations of **4**, one of which is shown in Figure 4. The dibenzothiophene part of PyDBT is oriented toward the η^6-benzene ligand, unlike the κ^1S-coordinated dibenzothiophenes in $[CpRu(CO)_2(DBT\text{-}\kappa^1S)]BF_4$ and $[CpRu(CO)_2(DBTh\text{-}\kappa^1S)]BF_4$, where DBTh represents 4-MeDBT, 4,6-Me$_2$DBT, and 2,8-Me$_2$DBT.[7h,i] To the best of our knowledge this is the first example of the structurally characterized complex of dibenzothiophene derivatives that has a six-membered N,S-chelate ring, although (*S*)-dibenzothiophene-4-yl-4-isopropyloxazoline was used as an N,S-chelate ligand for the Pd catalyst.[17] The Ru−S distances of **4** (2.3821(9) and 2.3901(8) Å) are close to those of the ruthenium(II) complexes with the κ^1S-coordinated dibenzothiophenes (2.377(2)−2.400(1) Å).[7h,i] The dihedral angle of the pyridyl group and the attached benzene ring in the dibenzothiophene part is 37.7(2)°, which largely deviates from the planar structure of the free PyDBT ligand in the crystal. These structural features imply that the pyridyl-substituted dibenzothiophene is flexible enough to bind metal ions by N,S-chelation.

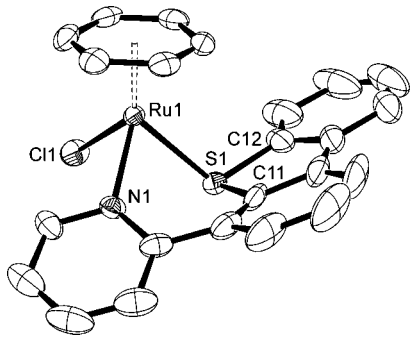

Figure 4. ORTEP drawing of **4** with thermal ellipsoids at the 50% probability level. Hydrogen atoms are omitted for clarity. Selected bond lengths (Å) and angles (deg): Ru(1)−S(1) 2.3821(9), Ru(1)−Cl(1) 2.3847(10), Ru(1)−N(1) 2.161(3), S(1)−C(11) 1.762(5), S(1)−C(12)1.757(3),Ru(1)−C(arene)2.178(3)−2.204(4),S(1)−Ru(1)−Cl(1) 82.84(3), S(1)−Ru(1)−N(1) 79.20(7), N(1)−Ru(1)−Cl(1) 88.28(9), C(11)−S(1)−C(12) 91.1(2).

Isomerization of 1b to 1a. Complexes **1a** and **1b** are fairly stable in solution, as expected from the reaction conditions. The ^{1}H NMR spectrum of the toluene-d_8 solution of **1b** slowly changed to that of **1a** at 100 °C (25% conversion for 7 h) with a small amount of unidentified species. This indicates that the C_2 isomer **1b** is converted to the thermodynamically stable C_i isomer **1a**. The crystal structures of **1a** and **1b** suggest that the steric repulsion between two PyBPT ligands exists in **1b** rather than **1a**. The isomerization in DMSO-d_6 at 80 °C (70% conversion for 3 h) was much faster than that in toluene-d_8.[16] Moreover, **1a** has different chiralities at the two Ru centers in a molecule, while **1b** has the same chiralities. Thus, **1b** would undergo cleavage of Ru−S bonds in the isomerization with altering the combination of the chiralities at the Ru centers, which implies that the Ru(PyBPT)$(CO)_2$ unit behaves like a mononuclear pincer complex during the reaction.

The C_2 isomer of **2** was also isomerized to its C_i isomer in DMSO-d_6 at 80 °C. ^{1}H NMR signals of the C_2 isomer disappeared within 2 h, and new signals appeared. The spectrum after heating for 5 h indicated that there are two kinds of coordinated ligands, and one of them corresponded well to the C_i isomer **1a** except for the 4-positioned methyl group. The C_2 isomers for **1** and **2** would be kinetic products and survive under the reaction conditions because of the low solubility.

Reaction of $[Rh(\mu\text{-}Cl)(CO)_2]_2$ with PyDBT. A higher efficiency in C−S activation induced by the coordination of the pyridyl group was found in the reaction with $[Rh(\mu\text{-}Cl)(CO)_2]_2$. Although no change was observed in the ^{1}H NMR spectrum of the toluene-d_8 solution containing dibenzothiophene and $[Rh(\mu\text{-}Cl)(CO)_2]_2$ after heating at 100 °C for 12 h, cyclometalation via C−S bond cleavage proceeded for PyDBT as described below (Scheme 3). Furthermore, stepwise formation of the thiametallacycle was observed.

The reaction of $[Rh(\mu\text{-}Cl)(CO)_2]_2$ (1 equiv) with PyDBT (2 equiv) in dichloromethane readily produced the mononuclear

(16) Details are given in the Supporting Information.
(17) Voituriez, A.; Schlz, E. *Tetrahedron: Asymmetry* **2003**, *14*, 339–346.

Scheme 3

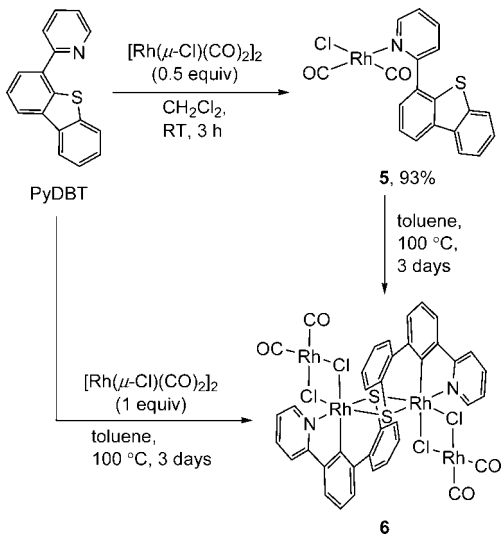

rhodium(I) complex *cis*-[RhCl(CO)$_2$(η^1-*N*-PyDBT)] (**5**, 93% yield). The single-crystal X-ray structure analysis of **5** revealed that PyDBT is bound to Rh through the pyridyl N atom, retaining the cis structure from the [Rh(μ-Cl)(CO)$_2$]$_2$ dimer (Figure 5). The Rh−N bond distance (2.114(5) Å) is very close to that in *cis*-[RhCl(CO)$_2$(py)] (2.122(7) Å).[18] The dihedral angle between the pyridine ring and the plane defined by Rh(1), Cl(1), C(1), and C(2) is 61.08(17)°, which is larger than that found for *cis*-[RhCl(CO)$_2$(py)] (39°), and the N(1)−Rh(1)−C(1) angle is 172.3(2)°. The structural deviation is related to the steric bulk of a dibenzothiophene-4-yl group in PyDBT.

Heating a toluene solution of **5** at 100 °C for 3 days provided an orange precipitate of [{Rh(μ-PyBPT-κ^3*N,C,S*)}(μ-Cl)$_2$-{Rh(CO)$_2$}]$_2$ (**6**) in 44% yield based on Rh. The elemental analysis was consistent with the formula Rh(PyBPT)Cl$_2$Rh(CO)$_2$, and the dinuclear core structure of {Rh(PyBPT)}$_2$ was predicted by the ESI mass spectrum, which shows two sets of peaks at m/z = 762.91 and 956.79 corresponding to [{Rh(PyBPT)}$_2$Cl]$^+$ and [{Rh(PyBPT)}$_2$RhCl$_2$(CO)$_2$]$^+$, respectively.

The structure of **6** was confirmed by single-crystal X-ray analysis. The asymmetric unit consists of two half-molecules of **6** and a toluene molecule. One of two complex molecules is shown in Figure 6, and selected bond lengths and angles are

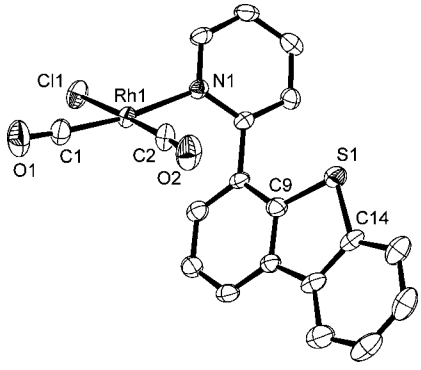

Figure 5. ORTEP drawing of **5** with thermal ellipsoids at the 50% probability level. Hydrogen atoms are omitted for clarity. Selected bond lengths (Å) and angles (deg): Rh(1)−Cl(1) 2.3368(15), Rh(1)−N(1) 2.114(5), Rh(1)−C(1) 1.843(7), Rh(1)−C(2) 1.831(5), S(1)−C(9) 1.767(6), S(1)−C(14) 1.755(5), Cl(1)−Rh(1)−N(1) 88.50(11), Cl(1)−Rh(1)−C(1) 89.07(18), Cl(1)−Rh(1)−C(2) 178.0(2), N(1)−Rh(1)−C(1)172.3(2), N(1)−Rh(1)−C(2) 93.2(2), C(1)−Rh(1)−C(2) 89.4(3), C(9)−S(1)−C(14) 91.6(2).

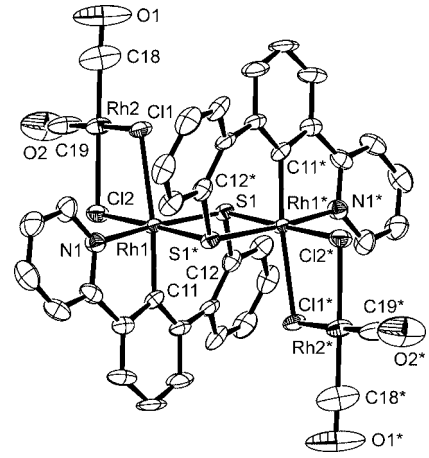

Figure 6. ORTEP drawing of **6** with thermal ellipsoids at the 50% probability level. Hydrogen atoms are omitted for clarity.

Table 2. Selected Bond Lengths (Å) and Angles (deg) for 6

Rh(1)−Cl(1)	2.5860(18)	Rh(3)−Cl(3)	2.5852(19)
Rh(1)−Cl(2)	2.440(2)	Rh(3)−Cl(4)	2.4379(17)
Rh(1)−S(1)	2.2882(18)	Rh(3)−S(2)	2.291(2)
Rh(1)−S(1*)	2.306(2)	Rh(3)−S(2*)	2.3070(15)
Rh(1)−N(1)	2.050(5)	Rh(3)−N(2)	2.056(7)
Rh(1)−C(11)	1.976(6)	Rh(3)−C(30)	1.983(7)
Rh(2)−Cl(1)	2.357(2)	Rh(4)−Cl(3)	2.3608(17)
Rh(2)−Cl(2)	2.3523(18)	Rh(4)−Cl(4)	2.351(2)
Rh(2)−C(18)	1.833(10)	Rh(4)−C(37)	1.823(11)
Rh(2)−C(19)	1.838(11)	Rh(4)−C(38)	1.847(8)
S(1)−C(12)	1.777(7)	S(2)−C(31)	1.792(6)
Rh(1)···Rh(1*)	3.4409(10)	Rh(3)···Rh(3*)	3.4395(8)
Rh(1)···Rh(2)	3.5890(8)	Rh(3)···Rh(4)	3.5907(8)
Cl(1)−Rh(1)−Cl(2)	80.93(7)	Cl(3)−Rh(3)−Cl(4)	80.94(5)
S(1)−Rh(1)−N(1)	171.5(2)	S(2)−Rh(3)−N(2)	171.55(15)
S(1)−Rh(1)−C(11)	85.1(2)	S(2)−Rh(3)−C(30)	94.9(2)
N(1)−Rh(1)−C(11)	82.5(2)	N(2)−Rh(3)−C(30)	82.3(3)
S(1)−Rh(1)−S(1*)	82.99(7)	S(2)−Rh(3)−S(2*)	83.16(7)
Cl(1)−Rh(2)−Cl(2)	87.74(7)	Cl(3)−Rh(4)−Cl(4)	87.63(6)
Rh(1)−Cl(1)−Rh(2)	93.00(7)	Rh(3)−Cl(3)−Rh(4)	92.99(6)
Rh(1)−Cl(2)−Rh(2)	96.98(9)	Rh(3)−Cl(4)−Rh(4)	97.13(6)
Rh(1)−S(1)−Rh(1*)	97.01(6)	Rh(3)−S(2)−Rh(3*)	96.84(7)
Rh(1)−S(1)−C(12)	109.3(3)	Rh(3)−S(2)−C(31)	109.2(3)

listed in Table 2. The thiolato-bridged {Rh(PyBPT)}$_2$ unit bearing the tridentate-*N,C,S* coordination was found in **6**, giving a C_i symmetrical structure similar to **1a**. The remaining coordination sites are occupied by Cl ligands from two [RhCl$_2$(CO)$_2$]$^-$ units to form the mixed-valent tetranuclear rhodium(I/III/III/I) structure of [{Rh(μ-PyBPT-κ^3*N,C,S*)}(μ-Cl)$_2${Rh(CO)$_2$}]$_2$. The Rh−C(carbanion) (1.976(6) and 1.983(7) Å) and Rh−N (2.050(5) and 2.056(7) Å) bond lengths in **6** are close to those in bis(2-phenylpyridine)rhodium(III) units in the chloro-bridged dirhodium(III/I) complex [(ppy)$_2$Rh(μ-Cl)$_2$Rh(cod)], 1.981(4) and 2.045(4) Å (average), respectively.[19] On the other hand, the Rh−C(carbanion) bond length in **6** is slightly shorter than that in [Cp*Rh(μ-SC$_{12}$H$_8$)]$_2$ (Rh−C, 2.059(5) Å (trans form), 2.021(7) Å (cis form)),[7a] which is presumably partially due to the additional chelate structure by the 2-phenylpyridine unit. The biphenyl twists of 26.0(3)° and 25.9(3)° in **6** are the smallest among the complexes with PyBPT-κ^3*N,C,S* ligands.

Formation Mechanism of 6. Complex **6** has two additional RhCl(CO)$_2$ units in the tetranuclear structure than in the dimeric

(18) Heaton, B.; Jacob, C.; Sampanthar, J. T. *J. Chem. Soc., Dalton Trans.* **1998**, 1403–1410.
(19) Polborn, K.; Severin, K. *Eur. J. Inorg. Chem.* **1998**, 1187–1192.

Scheme 4. Proposed Mechanism for the Formation of 6

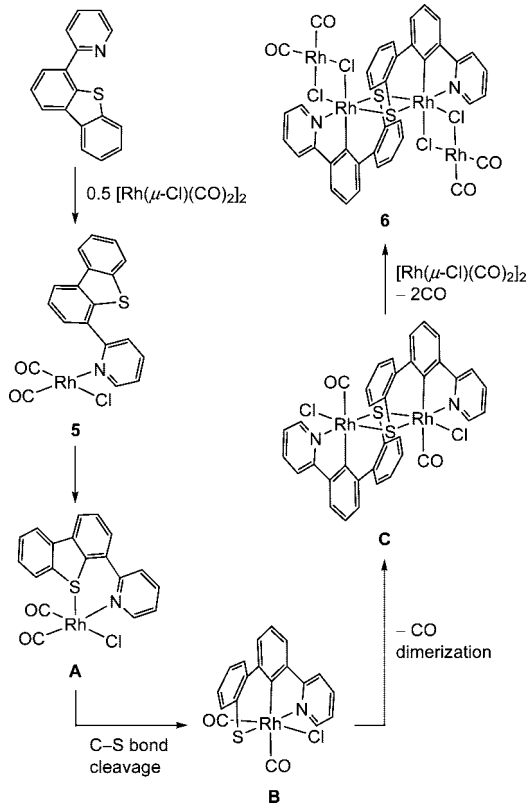

structure of $\{Rh(\mu\text{-PyBPT-}\kappa^3N,C,S)Cl\}_2$. The direct reaction using $[Rh(\mu\text{-Cl})(CO)_2]_2$ (1 equiv) and PyDBT (2 equiv) without isolation of **5** also gave **6** in 52% yield based on Rh, but theoretically wastes 50% of PyDBT. Indeed, the corresponding 1:1 reaction yielded twice the amount of **6** (yield: 56% based on Rh), suggesting the importance of a $RhCl(CO)_2$ unit in the formation of **6**. Interestingly, the CO ligands are completely released from the $\{Rh(PyBPT)\}_2$ unit in this reaction, which might provide a useful route to the more reactive pincer-type complex with the Rh(PyBPT-κ^3N,C,S) core structure.

A possible formation mechanism of **6** is shown in Scheme 4. The first step is the formation of the N-bound PyDBT complex **5** by the reaction of PyDBT with 0.5 equiv of $[Rh(\mu\text{-Cl})(CO)_2]_2$, which was confirmed by the X-ray crystal structure analysis as described above. Subsequently, the PyDBT-κ^2N,S complex **A** forms, and then the rhodium ion is inserted into the C−S bond to afford the PyBPT-κ^3N,C,S pincer-type complex **B**. After elimination of CO, the vacant site is filled by a lone pair on a thiolato S donor from another complex, **B**, to afford the dimeric intermediate **C**, containing a thiolato-bridged Rh_2S_2 core, which is similar to complex **1a**. The monomeric unit of $[Rh(\mu\text{-Cl})(CO)_2]_2$ reacts with intermediate **C** with the second elimination of CO to give the mixed-valent tetranuclear rhodium(I/III/III/I) complex **6**.

Conclusions

The metal-mediated C−S bond cleavage of pyridyl-substituted dibenzothiophenes, PyDBT, 4-MePyDBT, and 6-MePyDBT, provided thiolate-containing NCS pincer frameworks. The pyridyl group significantly affects the reactivity of dibenzothiophenes. Regioselective C−S bond activation was observed in the reaction using $[Ru_3(CO)_{12}]$ to afford the PyBPT-κ^3N,C,S diruthenium(II) complexes **1**, **2**, and **3**. The lower reactivity of 6-MePyDBT indicates that the initial coordination of the pyridyl group is important in the formation of the C−S cleaved products. Furthermore, the stepwise reaction via the η^1-*N*-PyDBT rhodium(I) complex **5** was observed in the formation of the tetranuclear rhodium(I/III/III/I) complex **6**. The precoordination of the pyridyl group, including the N,S-chelating mode, accelerates the oxidative addition of the C−S bond by increasing the accessibility of the C−S bond to the vacant site on the metal center. While further studies are required for a mechanistic understanding, the synthetic procedure presented here is useful for developing thiolate-containing metallacycle compounds.

Experimental Section

General Procedures. All manipulations were performed using a glovebox under an atmosphere of oxygen-free dry argon or standard Schlenk techniques under argon. Dried solvents and $[Pd(PPh_3)_4]$ were purchased from Nacalai Tesque, Inc. Dibenzothiophene was purchased from Tokyo Chemical Industry Co., Ltd. Triruthenium dodecacarbonyl was purchased from Aldrich Chemical Co. The compounds $[RuCl_2(\eta^6\text{-}C_6H_6)]_2$,[20] $[RhCl(CO)_2]_2$,[21] and dibenzothiophene-4-boronic acid[22] were prepared according to literature procedures. NMR spectra were recorded on a JEOL Lambda 300, a Bruker AVANCE 300, or a Bruker AVANCE 600 FT-NMR spectrometer at room temperature. IR spectra were obtained on a JASCO FT/IR-6200 spectrometer at room temperature. ESI mass spectrometry was performed on an Applied Biosystem Mariner time-of-flight mass spectrometer. Elemental analyses were performed by the Analytical Research Service Center at Osaka City University on Perkin-Elmer 240C or FISONS Instrument EA108 elemental analyzers.

Synthesis of 4-(2′-Pyridyl)dibenzothiophene (PyDBT).[12c] 2-Bromopyridine (1.74 g, 11.0 mmol) and dibenzothiophene-4-boronic acid (2.51 g, 11.0 mmol) were placed in a two-necked round-bottom flask. A deoxygenated solution of K_2CO_3 (2.10 g, 15.2 mmol) in dimethoxyethane/H_2O (200 mL, 3:1) was added to the flask. The mixture was stirred at room temperature, and then $[Pd(PPh_3)_4]$ (0.12 g, 0.11 mmol) was added. The reaction mixture was stirred at 100 °C for 6 h. The resulting yellow solution was extracted with chloroform (50 mL × 2). The chloroform layers were combined, dried over anhydrous $MgSO_4$, and filtered. The filtrate was concentrated to dryness, and the residue was purified by column chromatography (silica gel, 3 cm × 33 cm, dichloromethane/hexane, 2:1), affording a colorless powder. Recrystallization from hot methanol gave pure PyDBT as colorless crystals (2.31 g, 80%). ^1H NMR (600 MHz, $CDCl_3$): δ 8.86 (d, J = 4.3 Hz, 1H, 6-py), 8.25 (d, J = 7.7 Hz, 1H, 1-DBT), 8.19 (m, 1H, 9-DBT), 7.99 (d, J = 7.5 Hz, 1H, 3-DBT), 7.97 (d, J = 8.0 Hz, 1H, 3-py), 7.91 (m, 1H, 6-DBT), 7.81 (td, J = 7.7, 1.5 Hz, 1H, 4-py), 7.58 (t, J = 7.7 Hz, 1H, 2-DBT), 7.46 (m, 2H, 7-DBT, 8-DBT), 7.29 (m, 1H, 5-py). $^{13}C\{^1H\}$ NMR (151 MHz, $CDCl_3$): δ 156.2 (2-py), 148.5 (6-py), 142.0 (5a-DBT), 137.7 (4a-DBT), 137.3 (9b-DBT), 136.6 (4-py), 134.8 (9a-DBT), 133.4 (4-DBT), 126.7 (8-DBT), 125.0 (3-DBT), 124.5 (2-DBT), 124.1 (7-DBT), 122.4 (6-DBT), 122.13 (5-py), 122.08 (1-DBT), 121.3 (9-DBT), 120.9 (3-py). Anal. Calcd for $C_{17}H_{11}NS$: C 78.13, H 4.24, N 5.36. Found: C 77.87, H 4.12, N 5.36. MS (ESI^+): m/z = 261.1 ($[M]^+$).

Synthesis of 4-(4′-Methyl-2′-pyridyl)dibenzothiophene (4-MePyDBT). 2-Bromo-4-picoline (0.377 g, 2.2 mmol) and dibenzothiophene-4-boronic acid (0.50 g, 2.2 mmol) were placed in a two-necked round-bottom flask. A deoxygenated solution of K_2CO_3 (0.435 g, 3.15 mmol) in dimethoxyethane/H_2O (30 mL, 3:1) was added to the flask. The mixture was stirred at room temperature, and then $[Pd(PPh_3)_4]$ (0.025 g, 0.022 mmol) was added. The reaction

(20) Bennett, M. A.; Smith, A. K. *J. Chem. Soc., Dalton Trans.* **1974**, 233–241.
(21) McCleverty, J. A.; Wilkinson, G. *Inorg. Synth.* **1966**, *8*, 211–214.
(22) Reich, H. J.; Gudmundsson, B. Ö.; Green, D. P.; Bevan, M. J.; Reich, I. L. *Helv. Chim. Acta* **2002**, *85*, 3748–3772.

Table 3. Crystallographic Data for PyDBT, 1a, 1b, and 2

	PyDBT	1a	1b	2
empirical formula	$C_{17}H_{11}NS$	$C_{38}H_{22}N_2O_4Ru_2S_2$	$C_{38}H_{22}N_2O_4Ru_2S_2$	$C_{40}H_{26}N_2O_4Ru_2S_2$
fw	261.34	836.86	836.86	864.92
temperature, K	193	193	193	193
wavelength, Å	0.7107	0.7107	0.7107	0.7107
cryst syst	monoclinic	triclinic	monoclinic	triclinic
space group	$P2_1/a$	$P\bar{1}$	$C2/c$	$P\bar{1}$
a, Å	8.556(3)	8.805(3)	13.914(3)	10.3493(15)
b, Å	25.215(8)	9.666(4)	14.785(3)	11.1995(19)
c, Å	17.964(6)	10.320(4)	15.399(3)	16.002(2)
α, deg	90	105.377(9)	90	110.508(3)
β, deg	97.518(8)	91.151(4)	93.228(5)	90.7240(16)
γ, deg	90	109.159(8)	90	107.414(3)
V, Å^3	3842(2)	794.4(5)	3162.9(10)	1643.2(4)
Z	12	1	4	2
density (calcd), Mg/m^3	1.355	1.749	1.757	1.748
absorp coeff, mm^{-1}	0.235	1.129	1.134	1.094
F(000)	1632	416	1664	864
cryst size, mm^3	0.20 × 0.10 × 0.10	0.20 × 0.20 × 0.10	0.20 × 0.20 × 0.10	0.21 × 0.08 × 0.08
θ range, deg	4.0−27.5	4.1−27.5	4.0−27.5	4.0−27.5
index ranges	$-11 \le h \le 9$	$-11 \le h \le 9$	$-18 \le h \le 14$	$-12 \le h \le 13$
	$-32 \le k \le 28$	$-10 \le k \le 12$	$-16 \le k \le 19$	$-12 \le k \le 14$
	$-23 \le l \le 23$	$-13 \le l \le 11$	$-19 \le l \le 19$	$-20 \le l \le 20$
no. of reflns collected	37 313	7593	14 895	15 307
no. of indep rflns	8644 (R_{int} = 0.125)	3412 (R_{int} = 0.025)	3556 (R_{int} = 0.038)	6917 (R_{int} = 0.020)
completeness to θ	98.1% (θ = 27.48°)	93.4% (θ = 27.48°)	97.9% (θ = 27.48°)	91.6% (θ = 27.48°)
max. and min. transmn	0.977 and 0.648	0.893 and 0.841	0.893 and 0.794	0.916 and 0.751
no. of data/restraints/params	8644/0/574	3412/0/261	3556/0/228	6917/0/477
goodness of fit on F^2	1.072	1.023	1.000	1.015
final R indices [$I > 2\sigma(I)$]	R1 = 0.0564	R1 = 0.0308	R1 = 0.0280	R1 = 0.0280
R indices (all data)	wR2 = 0.0651	wR2 = 0.0785	wR2 = 0.0568	wR2 = 0.0810
largest diff peak and hole, e Å^{-3}	1.75 and −1.20	0.62 and −0.59	0.56 and −0.68	1.11 and −0.59

mixture was stirred at 100 °C overnight. The resulting yellow solution was extracted with chloroform (20 mL × 2). The chloroform layers were combined, dried over anhydrous $MgSO_4$, and filtered. The filtrate was concentrated to dryness, and the residue was purified by column chromatography (silica gel, dichloromethane/hexane, 2:1), affording a colorless powder. Recrystallization from hot methanol gave pure 4-MePyDBT as colorless crystals (0.20 g, 33%). ^{1}H NMR (600 MHz, $CDCl_3$): δ 8.73 (d, J = 4.9 Hz, 1H, 6-py), 8.24 (dd, J = 7.7 Hz, 1H, 1-DBT), 8.20 (m, 1H, 9-DBT), 7.99 (d, J = 7.4 Hz, 1H, 3-DBT), 7.93 (m, 1H, 6-DBT), 7.78 (s, 1H, 3-py), 7.58 (t, J = 7.7 Hz, 1H, 2-DBT), 7.47 (m, 2H, 7-DBT, 8-DBT), 7.12 (d, J = 4.9 Hz, 1H, 5-py), 2.45 (s, 1H, Me). ^{13}C{^{1}H} NMR (151 MHz, $CDCl_3$): δ 156.1 (2-py), 148.2 (6-py), 147.7 (4-py), 142.0 (5a-DBT), 137.7 (4a-DBT), 137.1 (9b-DBT), 134.8 (9a-DBT), 133.5 (4-DBT), 126.7 (7-DBT), 125.0 (3-DBT), 124.5 (2-DBT), 124.0 (8-DBT), 123.2 (5-py), 122.4 (6-DBT), 121.9 (1-DBT), 121.8 (3-py), 121.3 (9-DBT), 21.3 (CH_3). Anal. Calcd for $C_{18}H_{13}NS$: C 78.51, H 4.76, N 5.09. Found: C 78.15, H 4.75, N 5.02. MS (ESI$^+$): m/z = 276.1 ([M + H]$^+$).

Synthesis of 4-(6′-Methyl-2′-pyridyl)dibenzothiophene (6-MePyDBT). 2-Bromo-6-picoline (0.24 mL, 2.2 mmol) and dibenzothiophene-4-boronic acid (0.50 g, 2.2 mmol) were placed in a two-necked round-bottom flask. A deoxygenated solution of K_2CO_3 (0.435 g, 3.15 mmol) in dimethoxyethane (27 mL) and H_2O (7.5 mL) was added to the flask. The mixture was stirred at room temperature, and then [$Pd(PPh_3)_4$] (0.010 g, 0.0087 mmol) was added. The reaction mixture was stirred at 100 °C overnight. The resulting yellow solution was extracted with chloroform (20 mL × 2). The chloroform layers were combined, dried over anhydrous $MgSO_4$, and filtered. The filtrate was concentrated to dryness, and the residue was purified by column chromatography (silica gel, dichloromethane), affording a pale yellow powder. Recrystallization from hot methanol gave pure 6-MePyDBT as pale yellow crystals (0.38 g, 63%). ^{1}H NMR (600 MHz, $CDCl_3$): δ 8.23 (d, J = 7.6 Hz, 1H, 1-DBT), 8.19 (m, 1H, 9-DBT), 7.99 (d, J = 7.4 Hz, 1H, 3-DBT), 7.93 (m, 1H, 6-DBT), 7.77 (d, J = 7.9 Hz, 1H, 3-py), 7.70 (t, J = 7.7 Hz, 1H, 4-py), 7.56 (t, J = 7.6 Hz, 1H, 2-DBT), 7.46 (m, 2H, 7-DBT, 8-DBT), 7.13 (d, J = 7.5 Hz, 1H, 5-py), 2.77 (s, 3H, CH_3). ^{13}C{^{1}H} NMR (151 MHz, $CDCl_3$): δ 157.6 (6-py), 155.3 (2-py), 142.4 (5a-DBT), 137.8 (4a-DBT), 137.3 (9b-DBT), 136.9 (4-py), 134.8 (9a-DBT), 133.5 (4-DBT), 126.6 (7-DBT), 124.8 (3-DBT), 124.5 (2-DBT), 124.0 (8-DBT), 122.4 (6-DBT), 121.9 (1-DBT), 121.5 (5-py), 121.3 (9-DBT), 117.7 (3-py), 24.1 (CH_3). Anal. Calcd for $C_{18}H_{13}NS$: C 78.51, H 4.76, N 5.09. Found: C 78.17, H 4.72, N 5.09. MS (ESI$^+$): m/z = 276.1 ([M + H]$^+$).

Synthesis of [Ru(μ-PyBPT-κ^3*N,C,S*)(CO)$_2$]$_2$ (1). A glass tube with a Teflon valve was charged with PyDBT (31.4 mg, 0.12 mmol), [$Ru_3(CO)_{12}$] (25.6 mg, 0.040 mmol), and toluene (10 mL). The tube was sealed, and then the orange suspension was stirred at 100 °C for 3 days, during which time a pale yellow precipitate appeared. The resulting yellow suspension was filtered, and the filtrate was placed at −20 °C for 1 day to give a pale yellow powder of **1b** (4 mg). The ^{1}H NMR spectrum and the elemental analysis indicated that the collected precipitate contains two isomers, **1a** and **1b**. Anal. Calcd for $C_{38}H_{22}N_2O_4Ru_2S_2$: C 54.54, H 2.65, N 3.35. Found: C 54.43, H 2.60, N 3.30. The solid containing **1a** and **1b** was added to dichloromethane (10 mL). The pale yellow insoluble solid (**1a**) was collected by filtration (18 mg, 36%), and the filtrate was evaporated to give a pale yellow powder of **1b** (15 mg). The total yield of **1b** was 19 mg (38%). **1a**: ^{1}H NMR (600 MHz, $(CD_3)_2SO$): δ 8.47 (d, J = 8.1 Hz, 1H, 3-py), 8.25 (d, J = 7.5 Hz, 1H, 4′-BPT), 8.15 (d, J = 5.2 Hz, 1H, 6-py), 8.08 (t, J = 7.7 Hz, 1H, 4-py), 7.91 (d, J = 7.7 Hz, 1H, 6′-BPT), 7.78 (d, J = 7.8 Hz, 1H, 6-BPT), 7.51 (t, J = 7.7 Hz, 1H, 5′-BPT), 7.25 (t, J = 7.2 Hz, 1H, 5-BPT), 7.18 (t, J = 6.1 Hz, 1H, 5-py), 6.76 (t, J = 7.1 Hz, 1H, 4-BPT), 5.99 (d, J = 7.3 Hz, 1H, 3-BPT). ^{13}C{^{1}H} NMR (151 MHz, $(CD_3)_2SO$): δ 196.9 (*C*O), 194.4 (*C*O), 175.7 (2′-BPT), 165.2 (2-py), 152.9 (6-py), 147.4 (3′-BPT), 145.3 (1-BPT), 142.7 (1′-BPT), 138.4 (4-py), 133.1 (2-BPT), 131.7 (3-BPT), 130.9 (6-BPT), 129.7 (6′-BPT), 127.4 (5-BPT), 125.5 (5′-BPT), 125.3 (4-BPT), 124.1 (4′-BPT), 123.0 (5-py), 121.0 (3-py). IR (KRS): ν_{CO} = 2015 (s), 1950 (s) cm^{-1}. Anal. Calcd for $C_{38}H_{22}N_2O_4Ru_2S_2$: C 54.54, H 2.65, N 3.35. Found: C 54.28, H

Table 4. Crystallographic Data for 4, 5, and 6

	4	5	6
empirical formula	$C_{24}H_{17}ClF_3NO_3RuS_2 \cdot 0.5CDCl_3$	$C_{19}H_{11}ClNO_2RhS$	$C_{45}H_{30}Cl_4N_2O_4Rh_4S_2$
fw	685.24	455.72	1280.30
temperature, K	193	193	193
wavelength, Å	0.7107	0.7107	0.7107
cryst syst	triclinic	monoclinic	triclinic
space group	$P\bar{1}$	$P2_1/c$	$P\bar{1}$
a, Å	13.923(2)	12.494(4)	10.4989(11)
b, Å	14.058(3)	11.358(3)	15.479(2)
c, Å	15.425(3)	13.889(5)	15.746(2)
α, deg	106.098(2)	90	77.245(14)
β, deg	95.814(2)	116.917(6)	70.566(13)
γ, deg	114.678(3)	90	70.183(13)
V, Å^3	2553.1(8)	1757.4(10)	2253.4(5)
Z	4	4	2
density (calcd), Mg/m^3	1.781	1.722	1.887
absorp coeff, mm^{-1}	1.091	1.252	1.811
F(000)	1364	904	1252
cryst size, mm^3	0.21 × 0.21 × 0.18	0.22 × 0.10 × 0.10	0.25 × 0.04 × 0.04
θ range, deg	4.1−27.5	4.0−27.5	4.0−27.5
index ranges	$-18 \le h \le 15$ $-14 \le k \le 18$ $-20 \le l \le 19$	$-14 \le h \le 16$ $-12 \le k \le 14$ $-18 \le l \le 18$	$-13 \le h \le 13$ $-17 \le k \le 20$ $-20 \le l \le 20$
no. of reflns collected	25 623	16 990	22 356
no. of indep rflns	11 342 (R_{int} = 0.030)	3977 (R_{int} = 0.087)	9742 (R_{int} = 0.051)
completeness to θ	96.9% (θ = 27.48°)	98.9% (θ = 27.47°)	94.2% (θ = 27.48°)
max. and min. transmn	0.822 and 0.784	0.882 and 0.780	0.930 and 0.723
no. of data/restraints/params	11 342/0/668	3977/0/237	9742/0/591
goodness of fit on F^2	1.073	1.013	1.005
final R indices [$I > 2\sigma(I)$]	R1 = 0.0430	R1 = 0.0544	R1 = 0.0568
R indices (all data)	wR2 = 0.1003	wR2 = 0.0909	wR2 = 0.1202
largest diff peak and hole, e Å^{-3}	1.01 and −1.16	2.89 and −2.49	2.11 and −1.62

2.67, N 3.29. **1b**: ^{1}H NMR (600 MHz, $(CD_3)_2SO$): δ 8.88 (d, J = 5.3 Hz, 1H, 6-py), 7.87 (t, J = 7.3 Hz, 1H, 4-py), 7.78 (d, J = 8.2 Hz, 1H, 3-py), 7.38−7.32 (m, 3H, 5-py, 4′-BPT, 6-BPT), 7.12 (d, J = 7.7 Hz, 1H, 6′-BPT), 7.04 (t, J = 7.6 Hz, 1H, 5-BPT), 6.97 (t, J = 7.7 Hz, 1H, 5′-BPT), 6.43 (d, J = 7.3 Hz, 1H, 4-BPT), 5.87 (d, J = 8.7 Hz, 1H, 3-BPT). ^{13}C{^{1}H} NMR (151 MHz, $(CD_3)_2SO$): δ 197.3 (*C*O), 194.0 (*C*O), 174.2 (2′-BPT), 164.2 (2-py), 153.2 (6-py), 145.8 (1-BPT), 145.7 (3′-BPT), 141.1 (1′-BPT), 137.8 (4-py), 133.2 (3-BPT), 130.2 (6′-BPT), 129.6 (6-BPT), 126.5 (5-BPT), 125.6 (2-BPT), 124.7 (4-BPT), 123.5 (5′-BPT), 123.3 (5-py), 123.1 (4′-BPT), 120.9 (3-py). IR (KRS): ν_{CO} = 2006 (s), 1949 cm^{-1} (s). Anal. Calcd for $C_{38}H_{22}N_2O_4Ru_2S_2$: C 54.54, H 2.65, N 3.35. Found: C 54.49, H 2.55, N 3.34.

Synthesis of [Ru(μ-4-MePyBPT-κ^3*N,C,S*)(CO)$_2$]$_2$ (2). A glass tube with a Teflon valve was charged with 4-MePyDBT (83 mg, 0.30 mmol), [$Ru_3(CO)_{12}$] (64 mg, 0.10 mmol), and toluene (15 mL). The tube was sealed, and then the orange suspension was stirred at 100 °C for 3 days, during which time a pale yellow crystalline precipitate appeared. The precipitate was collected by filtration. The yield of complex **2** was 68 mg (52%). ^{1}H NMR (300 MHz, $(CD_3)_2SO$): δ 8.71 (d, J = 5.8 Hz, 1H, 6-py), 7.63 (s, 1H, 3-py), 7.36 (d, J = 7.6 Hz, 1H, 4′-BPT), 7.34 (d, J = 7.6 Hz, 1H, 6-BPT), 7.22 (dd, J = 5.8, 1.1 Hz, 1H, 5-py), 7.10 (d, J = 7.7 Hz, 1H, 6′-BPT), 7.05 (td, J = 7.6, 1.5 Hz, 1H, 5-BPT), 6.96 (t, J = 7.7 Hz, 1H, 5′-BPT), 6.46 (td, J = 7.4, 1.2 Hz, 1H, 4-BPT), 5.92 (dd, J = 7.7, 1.4 Hz, 1H, 3-BPT), 2.42 (s, 3H, CH_3). IR (KRS): ν_{CO} = 2017 (s), 1958 cm^{-1} (s). Anal. Calcd for $C_{40}H_{26}N_2O_4Ru_2S_2$: C, 55.55; H, 3.03; N, 3.24. Found: C 55.53; H, 2.96; N, 3.12.

Synthesis of [Ru(μ-6-MePyBPT-κ^3*N,C,S*)(CO)$_2$]$_2$ (3). A glass tube with a Teflon valve was charged with 6-MePyDBT (33.0 mg, 0.12 mmol), [$Ru_3(CO)_{12}$] (25.6 mg, 0.040 mmol), and toluene (10 mL). The tube was sealed, and then the orange suspension was stirred at 100 °C for 3 days, during which time a pale yellow crystalline precipitate appeared. The precipitate was collected by filtration. The yield of complex **3** was 15 mg (29%). IR (KRS): ν_{CO} = 2018 (s), 1961 cm^{-1} (s). Anal. Calcd for $C_{40}H_{26}N_2O_4Ru_2S_2$: C, 55.55; H, 3.03; N, 3.24. Found: C, 54.70; H, 2.91; N, 3.14. This complex was dissolved in DMSO-d_6 at 80 °C, and a ^{1}H NMR spectrum (300 MHz, $(CD_3)_2SO$) was recorded. The chemical shifts of major signals are as follows: δ 8.35 (d, J = 8.0 Hz, 1H, 3-py), 8.23 (d, J = 7.3 Hz, 1H, 4′-BPT), 7.98 (t, J = 7.8 Hz, 1H, 4-py), 7.90 (d, J = 7.8 Hz, 1H, 6′-BPT), 7.83 (d, J = 7.9 Hz, 1H, 6-BPT), 7.47 (t, J = 7.8 Hz, 1H, 5′-BPT), 7.31−7.22 (m, 2H, 5-BPT, 5-py), 6.77 (td, J = 7.4, 1.2 Hz, 1H, 4-BPT), 5.98 (dd, J = 7.7, 1.4 Hz, 1H, 3-BPT), 2.17 (s, 1H, CH_3).

Synthesis of [Ru(η^6-C$_6$H$_6$)(PyDBT-κ^2*N,S*)Cl]CF$_3$SO$_3$ (4). [$RuCl_2(\eta^6$-$C_6H_6)]_2$ (90 mg, 0.18 mmol) and PyDBT (92 mg, 0.35 mmol) were dissolved in chloroform (12 mL), and $AgCF_3SO_3$ (90 mg, 0.35 mmol) was added. The brown suspension was filtered, and then the yellow filtrate was heated at 60 °C for 30 min in a glass tube with a Teflon valve. After standing the yellow solution at −30 °C for 3 days, reddish-orange crystals of **4** were deposited. Yield: 81 mg (37%). ^{1}H NMR (600 MHz, $CDCl_3$): δ 9.38 (d, J = 5.7 Hz, 1H, 6-py), 8.38 (d, J = 7.8 Hz, 1H, 9-DBT), 8.33 (d, J = 7.9 Hz, 1H, 1-DBT), 8.22 (d, J = 7.5 Hz, 1H, 3-DBT), 8.17−8.11 (m, 3H, 6-DBT, 3-py, 4-py), 7.93 (t, J = 7.7 Hz, 1H, 2-DBT), 7.89 (t, J = 7.6 Hz, 1H, 8-DBT), 7.75 (t, J = 7.6 Hz, 1H, 7-DBT), 7.63 (td, J = 6.1, 2.6 Hz, 1H, 5-py), 5.30 (s, 6H, η^6-C$_6H_6$). ^{13}C{^{1}H} NMR (151 MHz, $CDCl_3$): δ 157.7 (6-py), 157.0 (2-py), 140.7 (4-py), 139.2 (9a-DBT), 138.4 (5a-DBT), 136.7 (4a-DBT), 135.2 (4-DBT), 134.6 (9b-DBT), 131.2 (3-DBT), 130.8 (2-DBT), 130.7 (8-DBT), 129.8 (7-DBT), 126.1 (5-py), 125.72, 125.67 (6-DBT, 3-py), 124.3 (1-DBT), 124.1 (9-DBT), 87.1 (η^6-C_6H_6). Anal. Calcd for $C_{24}H_{17}ClF_3NO_3RuS_2 \cdot 0.1CHCl_3$: C, 45.44; H, 2.71; N, 2.20. Found: C, 45.55; H, 2.89; N, 2.25. Crystals suitable for X-ray structure analysis were grown from the $CDCl_3$ solution as the formula [Ru(η^6-C_6H_6)(η^2-*N,S*-PyDBT)Cl]$CF_3SO_3 \cdot 0.5CDCl_3$.

Synthesis of [RhCl(CO)$_2$(η^1-*N*-PyDBT)] (5). [$RhCl(CO)_2]_2$ (58 mg, 0.15 mmol) and PyDBT (78 mg, 0.30 mmol) were dissolved in dichloromethane (10 mL) and then stirred for 3 h. The yellow solution was layered with hexane and cooled at −30 °C for 1 week to obtain yellow crystals of **5** (126 mg, 93%). ^{1}H NMR (600 MHz, $CDCl_3$): δ 9.00 (d, J = 5.4 Hz, 1H, 6-py), 8.36 (d, J = 7.9 Hz, 1H, 1-DBT), 8.25 (d, J = 7.0 Hz, 1H, 9-DBT), 8.21 (d, J = 7.1 Hz,

1H, 3-DBT), 8.04 (t, $J = 7.4$ Hz, 1H, 4-py), 7.97 (d, $J = 7.7$ Hz, 1H, 3-py), 7.84 (d, $J = 7.3$ Hz, 1H, 6-DBT), 7.74 (t, $J = 7.6$ Hz, 1H, 2-DBT), 7.58 (t, $J = 6.0$ Hz, 1H, 5-py), 7.55−7.49 (m, 2H, 8-DBT, 7-DBT). $^{13}C\{^1H\}$ NMR (151 MHz, $CDCl_3$): δ 183.5 (d, $^1J_{RhC} = 62.2$ Hz, *C*O), 178.9 (d, $^1J_{RhC} = 72.1$ Hz, *C*O), 159.9 (2-py), 153.4 (6-py), 139.2 (4-py), 138.9 (5a-DBT), 138.3 (4a-DBT), 136.5 (9b-DBT), 135.3 (9a-DBT), 134.2 (4-DBT), 129.6 (3-DBT), 127.4 (7-DBT), 125.5 (3-py), 125.0 (2-DBT, 8-DBT), 124.5 (5-py), 123.4 (1-DBT), 122.8 (6-DBT), 122.0 (9-DBT). IR (KRS): $\nu_{CO} = 2073$ (s), 2004 cm^{-1} (s). MS (ESI^+): $m/z = 420.0$ ($[M - Cl]^+$). Anal. Calcd for $C_{19}H_{11}ClNO_2RhS \cdot 4CH_2Cl_2$: C 34.73, H 2.41, N 1.76. Found: C 35.05, H 2.36, N 1.62. Crystals suitable for X-ray structure analysis were grown from a toluene solution as the formula [RhCl(CO)$_2$(η^1-*N*-PyDBT)].

Synthesis of [Rh$_2$(μ-PyBPT-κ^3*N,C,S*)(μ-Cl)$_2$(CO)$_2$]$_2$ (6). A glass tube with a Teflon valve was charged with PyDBT (39 mg, 0.15 mmol), $[RhCl(CO)_2]_2$ (58 mg, 0.15 mmol), and toluene (10 mL). The tube was sealed, and then the yellow solution was stirred at 100 °C for 3 days, during which time an orange precipitate appeared. The resulting orange suspension was filtered, and a yellow-orange powder of **5** was obtained. Yield: 50 mg (56%). ^1H NMR (600 MHz, CD_2Cl_2): δ 8.99 (d, $J = 4.8$ Hz, 1H, 6-py), 8.22 (d, $J = 8.0$ Hz, 1H, 3-py), 8.06−8.01 (m, 2H, 4-py, 4′-BPT), 7.94 (d, $J = 7.9$ Hz, 1H, 6′-BPT), 7.80 (d, $J = 7.8$ Hz, 1H, 6-BPT), 7.50 (t, $J = 7.6$ Hz, 1H, 5′-BPT), 7.46 (td, $J = 7.6$, 1.3 Hz, 1H, 5-BPT), 7.30 (td, $J = 7.0$, 2.1 Hz, 1H, 5-py), 6.84 (td, $J = 7.4$, 1.1 Hz, 1H, 4-BPT), 6.26 (dd, $J = 7.7$, 1.1 Hz, 1H, 3-BPT). IR (KRS): $\nu_{CO} = 2079$ (s), 2009 cm^{-1} (s). MS (ESI^+): $m/z = 956.8$ ($[M - Cl_2Rh(CO)_2]^+$). Anal. Calcd for $C_{38}H_{22}Cl_4N_2O_4Rh_4S_2$: C 38.41, H 1.87, N 2.36. Found: C 38.31, H 2.00, N 2.32. Crystals suitable for X-ray structure analysis were grown from a toluene solution as the formula [Rh$_2$(μ-PyBPT-κ^3*N,C,S*)(μ-Cl)$_2$(CO)$_2$]$_2$·C$_6$H$_5$CH$_3$.

The corresponding 1:2 reaction of $[RhCl(CO)_2]_2$ (29 mg, 0.075 mmol) and PyDBT (39 mg, 0.15 mmol) yielded 23 mg of **6** (52%).

Complex **6** was also synthesized by heating a toluene solution of **5** (115 mg, 0.25 mmol) at 100 °C for 3 days. Yield: 33 mg (44%).

NMR Experiments for the Reaction of [Ru$_3$(CO)$_{12}$] with PyDBT. An NMR tube with a Teflon valve was charged with PyDBT (6.2 mg, 0.024 mmol), $[Ru_3(CO)_{12}]$ (5.1 mg, 0.008 mmol), and toluene-d_8 (0.5 mL). The tube was heated at 100 °C, and ^1H NMR measurements were performed. After 15 h, ^1H NMR spectra showed the presence of **1a**, **1b**, PyDBT, and unidentified species in the solution, and microcrystals of **1a** and **1b** were deposited.

Comparison between the Reactions of PyDBT and 6-MePyDBT toward [Ru$_3$(CO)$_{12}$]. An NMR tube with a Teflon valve was charged with PyDBT (7.8 mg, 0.030 mmol), $[Ru_3(CO)_{12}]$ (6.4 mg, 0.010 mmol), and toluene-d_8 (0.5 mL). Another tube was charged with 6-MePyDBT (8.3 mg, 0.030 mmol), $[Ru_3(CO)_{12}]$ (6.4 mg, 0.010 mmol), and toluene-d_8 (0.5 mL). These tubes were heated at 100 °C, and ^1H NMR measurements were performed.

Isomerization of 1b to 1a. A toluene-d_8 and a DMSO-d_6 solution of **1b** were heated at 100 and 80 °C, respectively, using an NMR tube with a Teflon valve. ^1H NMR measurements were performed to monitor the isomerization of **1b** to **1a**.

X-ray Crystal Structure Determination of PyDBT, 1a, 1b, 2, 4, 5, and 6. A single crystal of PyDBT, **1a**, **1b**, **2**, **4**, **5**, or **6** was mounted on a glass fiber. The diffraction data were collected on an AFC7/CCD Mercury diffractometer using the rotation method with 0.5° frame width and with 10 s exposure time per frame. The data were processed and corrected for Lorentz and polarization effects using CrystalClear software.[23] The analyses were carried out using the CrystalStructure 3.8 crystallographic software package.[24] Absorption corrections were applied using the Multi Scan method for PyDBT, **2**, and **6** or a numerical method for the others. The structures were solved using direct methods (SIR97[25] for PyDBT, **4**, **5**, and **6**; SIR92[26] for **1a**; SHELX-97[27] for **1b**; SIR2002[28] for **2**) and refined by full-matrix least-squares on F^2 using CRYSTALS,[29] except that SHELXL[27] was used for **4**. Crystallographic data are summarized in Tables 3 and 4. All non-hydrogen atoms were refined anisotropically. PyDBT contained disordered structures, and the site occupancy factors for sulfur atoms were varied to model the positional disorder. The occupancy factors of 0.50, 0.50, 0.92, 0.08, 0.90, and 0.10 were used for S1, S2, S3, S4, S5, and S6, respectively. All hydrogen atoms except for those in **1a** were located on calculated positions and refined as the riding model. Hydrogen atoms in **1a** were found in difference Fourier maps and refined isotropically.

Acknowledgment. This work was supported by a Grant-in-Aid for Scientific Research (No. 18350033) from the Ministry of Education, Culture, Sports, Science and Technology of Japan. We thank Dr. Matsumi Doe for assistance with NMR data.

Supporting Information Available: Data for NMR experiments and crystallographic data in CIF format for PyDBT, **1a**, **1b**, **2**, **4**, **5**, and **6**. This material is available free of charge via the Internet at http://pubs.acs.org.

OM8003916

(23) *CrystalClear*; Rigaku Corp.: Woodlands, TX, 1999.
(24) *Crystal Structure 3.8, Crystal Structure Analysis Package*; Rigaku and Rigaku/MSC, 2000−2006.
(25) Altomare, A.; Burla, M. C.; Camalli, M.; Cascarano, G. L.; Giacovazzo, C.; Guagliardi, A.; Moliterni, A. G. G.; Polidori, G.; Spagna, R. *J. Appl. Crystallogr.* **1999**, *32*, 115–119.
(26) Altomare, A.; Cascarano, G.; Giacovazzo, C.; Guagliardi, A.; Burla, M. C.; Polidori, G.; Camalli, M. *J. Appl. Crystallogr.* **1994**, *27*, 435.
(27) Sheldrick, G. M. *SHELX-97, Program for the Solution and Refinement of Crystal Structures*; University of Göttingen: Göttingen, Germany, 1997.
(28) Burla, M. C.; Camalli, M.; Carrozzini, G. L.; Cascarano, G.; Giacovazzo, C.; Polidori, G.; Spagna, R. *J. Appl. Crystallogr.* **2003**, *36*, 1103.
(29) Walkin, D. J.; Prout, C. K.; Carruthers, J. R.; Betteridge, P. W.; *CRYSALS*; Chemical Crystallography Laboratory: Oxford, UK, 1996.